Multiple resonance induced thermally activated delayed fluorescence: Effect of chemical modification

Xiaopeng Wang^{1,*,‡}, Siyu Gao^{2,‡}, Aizhu Wang³, Bo Wang¹ and Noa Marom^{2,4,5}

- ¹ Qingdao Institute for Theoretical and Computational Sciences, Institute of Frontier and Interdisciplinary Science, Shandong University, Qingdao, Shandong 266237, P. R. China
- ² Department of Materials Science and Engineering, Carnegie Mellon University, Pittsburgh, PA 15213, USA.
- ³ Collaborative Innovation Center of Technology and Equipment for Biological Diagnosis and Therapy in Universities of Shandong, Institute for Advanced Interdisciplinary Research (iAIR), University of Jinan, Jinan, 250022, P. R. China.
- ⁴ Department of Physics, Carnegie Mellon University, Pittsburgh, PA 15213, USA.
- ⁵ Department of Chemistry, Carnegie Mellon University, Pittsburgh, PA 15213, USA.
- * Author to whom any correspondence should be addressed.
- [‡] These authors contributed equally to this work.

E-mail: xiaopengwang@sdu.edu.cn

Supplementary Material for this article is available online

Abstract. Thermally activated delayed fluorescence (TADF) is the internal conversion of triplet excitons into singlet excitons via reverse intersystem crossing (RISC). It improves the efficiency of OLEDs by enabling the harvesting of nonradiative triplet excitons. Multiple resonance (MR) induced TADF chromophores exhibit an additional advantage of high color purity due to their rigid conformation. However, owing to the strict design rules there is a limited number of known MR-TADF chromophores. For applications in full-color high-resolution OLED displays, it is desirable to extend the variety of available chromophores and their color range. We computationally explore the effect of chemical modification on the properties of the MR-TADF chromophore quinolino[3,2,1-de]acridine-5,9-dione (QAD). QAD derivatives are evaluated based on several metrics: The formation energy is associated with the ease of synthesis; The spatial distribution of the frontier orbitals indicates whether a compound remains an MR-TADF chromophore or turns into a donoracceptor TADF chromophore; The change of the singlet excitation energy compared to the parent compound corresponds to the change in color; The energy difference between the lowest singlet and triplet states corresponds to the barrier to RISC; The reorganization energy is associated with the color purity. Based on these metrics, QAD-6CN is predicted to be a promising MR-TADF chromophore with a cyan hue. This demonstrates that computer simulations may aid the design of new MR-TADF chromophores by chemical modification.

1. Introduction

Organic light-emitting diodes (OLEDs) are widely used in displays and lighting [1, 2, 3]. Owing to spin statistics, only 25% of electrically generated excitons are in a singlet state and the remaining 75% are in a triplet state. The radiative decay of triplet excitons to the singlet ground state is forbidden by selection rules, limiting the lighting efficiency of OLEDs. Thus, utilization of triplet excitons is crucial to the design and development of a new generation of OLEDs. In the first conventional OLED device, which was fabricated in 1987, only singlet excitons could be utilized for fluorescence [4]. In so-called second generation OLEDs, phosphorescent heavy-metal complexes were used to harvest triplet excitons [1, 5, 6, 7]. Heavy metal atoms enhance spin-orbit coupling, which facilitates intersystem crossing (ISC) between states with different spin multiplicities. However, they are expensive and environmentally hazardous. generation" OLEDs are based on thermally activated delayed fluorescence (TADF) chromophores [8, 9, 10, 11, 12, 13]. TADF molecules have a small energy gap, ΔE_{ST} , between the lowest singlet excited state, S_1 , and the lowest triplet excited state, T_1 . This enables thermal activation of the formally spin-forbidden reverse intersystem crossing (RISC) process from the long-lived T_1 state to the radiative S_1 state, followed by a light emitting transition from S_1 to the ground state, S_0 . TADF chromophores may be metalorganic complexes [14, 15, 16], but advantageously, they may be purely organic molecules [9, 17, 18, 19] or molecular nanocrystals [20, 21, 22]. Purely organic TADF chromophores are cheaper and biocompatible, which is attractive for wearable devices and biomedical applications [18, 23]. The internal quantum efficiency (IQE) of TADF-based OLEDs may reach nearly 100% [24, 25], i.e. full conversion of all excitons into photons. In addition to their main application in OLEDs, TADF chromophores may also be used to enhance the efficiency of solar cells by upconversion of low-energy incident photons, which would otherwise be lost, into higher-energy photons, above the absorption threshold. Upconversion via triplet-triplet annihilation (TTA) takes place in mixtures of sensitizer and emitter chromophores [26, 27, 28, 29, 30]. TADF molecules may serve as sensitizers, converting low-energy singlet excitons into triplet excitons, which subsequently combine into higher-energy singlet excitons in the emitter[31, 32, 33, 34, 35].

The first reported purely organic TADF molecule was eosin in 1961 [8]. Therein, TADF was observed at elevated temperatures because an energy barrier of $\Delta E_{ST} = 0.37$ eV must be thermally overcome in the endothermic RISC process. In 2011, Adachi et al. demonstrated that spatially separating the highest occupied molecular orbital (HOMO) and the lowest unoccupied molecular orbital (LUMO) leads to a very small electron exchange energy and thus to a very small ΔE_{ST} , producing efficient TADF at room temperature [36]. They synthesized a donor-acceptor molecule, where the HOMO and LUMO were localized on the donor and acceptor moieties, respectively, exhibiting a small ΔE_{ST} of 0.11 eV and efficient TADF [36]. Since then, numerous donor-acceptor TADF molecules have been experimentally synthesized and/or theoretically proposed thanks to the variety of possibilities of combining different numbers and types of donor

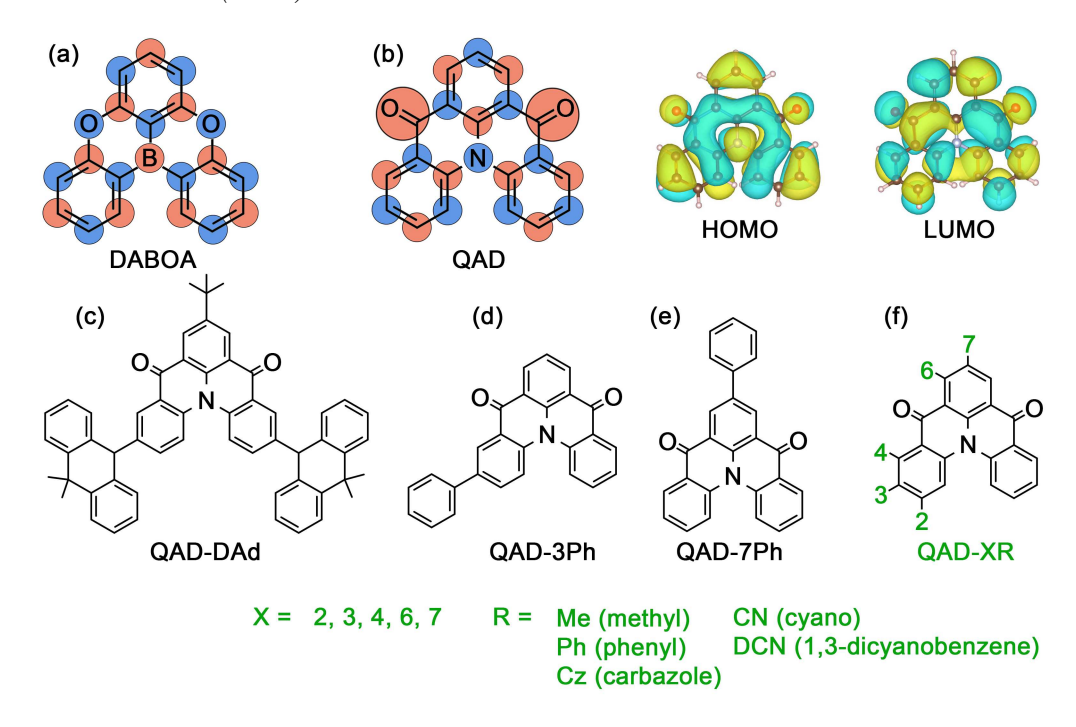


Figure 1. MR-TADF chromophores: (a) DABOA, (b) QAD and its frontier molecular orbitals visualized with an isosurface value of 0.014 au, (c) QAD-DAd, (d) QAD-3Ph, (e) QAD-7Ph, and (f) QAD-XR, where X indicates the C atom on the QAD skeleton where the chemical group R is attached.

and acceptor moieties [9, 12, 11, 10, 13, 19]. One drawback of donor-acceptor TADF molecules is their conformational flexibility, as they often contain rotatable single bonds between donor and acceptor moieties.[37] This may lead to a significant difference between the ground state geometry and the excited state geometry, resulting in a broad emission peak with a full width at half maximum (FWHM) typically ranging from 70 to 100 nm [9]. This poor color purity limits the application of TADF chromophores in high-resolution displays.

In 2015, Hatakeyama et al. proposed a new design strategy, harnessing multiple resonance (MR) induced TADF to significantly reduce the FWHM to about 30 nm [38, 39]. MR-TADF molecules are rigid "graphene flakes", comprising several six-membered rings doped with electron-donating atoms, such as N and O, and electron-withdrawing atoms, such as B. For example, the first reported MR-TADF molecule, 5,9-dioxa-13b-boranaphtho[3,2,1-de]anthracene (DABOA), is shown in Figure 1(a). O atoms and their second neighboring C atoms (indicated in blue) contribute to the HOMO, whereas the B atom and its second neighboring C atoms (indicated in red) contribute to the LUMO. The HOMO and LUMO are spatially separated on two groups of atoms due to the opposite resonance effect of O and B atoms, leading to a small ΔE_{ST} of 0.15 eV and the experimental observation of TADF [38]. Additional MR-TADF chromophores have been experimentally synthesized [40, 41, 42, 43, 44, 45, 46, 47, 48, 49, 50, 51], however their number is extremely limited compared to donor-acceptor TADF molecules. This is because the framework of MR-TADF molecules must be a conformationally rigid

small graphene flake. In addition, there is only one spatial arrangement of electron donating and withdrawing atoms, where each atom is surrounded by atoms of the opposite character. Furthermore, the electron donating and withdrawing atoms are, for the most part, limited to N or O, and B, respectively. One exception is quinolino[3,2,1-de]acridine-5,9-dione (QAD, also known as DiKTa or QAO), shown in Figure 1(b), where a carbonyl group serves as the electron withdrawing unit. The restricted design space of MR-TADF molecules limits their applications in both full-color high-resolution displays and TTA upconversion. For displays, a range of colors is desirable, which requires a variety of species with different S_1 energies. For TTA upconversion, it is desirable to reduce the energy loss and increase the anti-Stokes shift, which corresponds to the energy difference between the incident and upconverted photons. To this end, the T_1 energy of the TADF sensitizer should be as close as possible to the T_1 energy of the emitter molecule [31, 32, 33, 34, 35]. Therefore, MR-TADF molecules with different excitation energies are required to pair with different TTA emitters.

Chemical modification is a promising strategy for tuning the excitation energies of chromophores for diverse applications [9, 31, 33, 52, 53, 54]. This avenue has been explored in search of more MR-TADF molecules. For example, the 9-dimethyl-9,10dihydroacridine (DMAC) donor has been experimentally substituted onto QAD, yielding a new molecule, 7-(tert-butyl)-3,11-bis(9,9-dimethylacridin-10(9H)-yl)quinolino[3,2,1de acridine-5,9-dione (QAD-DAd), shown in Figure 1(c) [44]. However, QAD-DAd is a donor-acceptor TADF molecule rather than a MR-TADF molecule. The LUMO is still on the QAD framework, but the HOMO has shifted from the QAD framework to the two DMAC donor moieties. Due to the rotatable bonds between the QAD core and the DMAC moieties, the FWHM of the QAD-DAd emission peak is significantly broadened, leading to poor color purity compared to QAD [44]. additional phenylated QAD derivatives have been experimentally synthesized, namely 3-phenylquinolino[3,2,1-de]acridine-5,9-dione (QAD-3Ph) and 7-phenylquinolino[3,2,1delacridine-5,9-dione (QAD-7Ph) [45], shown in Figure 1(d) and (e). In contrast to QAD-DAd, QAD-3Ph and QAD-7Ph are fortunately still MR-TADF chromophores. The spatial distribution of their HOMOs and LUMOs on the QAD core is unchanged upon phenyl substitution. The only difference is that their HOMOs are extended over the additional phenyl rings [55]. The FWHMs of QAD-3Ph and QAD-7Ph are 30 and 22 nm, respectively, slightly smaller than the 32 nm of QAD [44, 45]. However, the S₁ energies of QAD, QAD-3Ph, and QAD-7Ph, estimated based on their absorption peaks, are 2.85, 2.80, and 2.78 eV, respectively, quite similar to each other [44, 45]. An effective route of chemical modification that would significantly tune the excitation energies of MR-TADF chromophores without turning them into donor-acceptor TADF chromophores is thus still missing.

We use computer simulations to investigate the effect of chemical modification on the excited-state properties of MR-TADF molecules. Density functional theory (DFT) [56] and time-dependent density functional theory (TDDFT) [57, 58] offer an appealing balance between accuracy and efficiency, as discussed in Section 3.1. We study QAD derivatives, denoted as QAD-XR, where X indicates the substitution position on the QAD skeleton and R indicates the substituent group, as shown in Figure 1(f). The QAD derivatives are evaluated based on several metrics. In Section 3.2, we evaluate the formation energy, which is associated with the ease of synthesis. In Section 3.3, we examine the spatial distribution of the frontier orbitals. In Section 3.4, we evaluate the excited-state properties of the QAD derivatives, including the change of the singlet excitation energy compared to the parent compound, which corresponds to the change in color, the energy difference between the lowest singlet and triplet states, ΔE_{ST} , which corresponds to the barrier to RISC, and the reorganization energy, which is associated with the color purity. Based on these metrics, QAD-6CN is predicted to be a promising MR-TADF chromophore with a cyan hue. The ΔE_{ST} and reorganization energy of QAD-6CN are comparable to those experimentally observed MR-TADF chromophores. The case study of QAD derivatives may be instructive for the development of new MR-TADF chromophores by chemical modification. This may help extend the range of available colors of MR-TADF chromophores and improve their performance.

2. Computational Details

All calculations were performed with version 5.0.0 of the ORCA code [59]. Ground state and excited state geometries were optimized with the ω B97X-D functional [60], which includes empirical pairwise dispersion corrections [61]. Def2-TZVP basis sets [62] were employed and tight SCF convergence criteria corresponding to an energy tolerance of 1×10^{-8} au were used. Atomic positions were fully relaxed until the maximal force was below 3×10^{-4} au. Optimized geometries were used in excited state calculations. TDDFT calculations were performed using the def2-TZVP basis sets [62]. Reference were performed using the domain-based local pair natural orbital (DLPNO) implementation [63, 64] of the similarity transformed equation of motion coupled cluster theory with single and double excitations (DLPNO-STEOM-CCSD) [65]. DLPNO-STEOM-CCSD calculations of QAD, QAD-3Ph, and QAD-7Ph were performed using the def2-TZVP basis sets [62]. The resolution of identity (RI) approximation was used with the def2-TZVP/C auxiliary basis sets [66]. The truncation parameter for singles pair natural orbitals (PNOs) was $1 \cdot 10^{-11}$, and the active space selection thresholds for occupied and virtual orbitals were set to $5 \cdot 10^{-3}$ [67].

3. Results and discussion

3.1. Performance of TDDFT

TDDFT is a formally exact theory of excited state. However, its predictive power strongly depends on the choice of approximation for the exchange-correlation (xc) functional. With semi-local functionals, the self-interaction error (SIE) affects the DFT orbital energies and further propagates to the TDDFT excited states, leading to energy underestimation of charge-transfer (CT) excitations, where electron and hole

are spatially separated [68, 69, 70]. The effect of SIE may be mitigated by mixing a fraction of range-separated exact (Fock) exchange with the semi-local exchange and correlation [71, 72, 73, 74, 75, 76, 77]. Functionals with 100% Fock exchange in the long range and a range separation parameter of about 0.30 $bohr^{-1}$ have been shown to provide a balanced description between valence and CT excitations [75]. This includes the long-range corrected (LC) hybrid functionals LC-BLYP [78] and ω B97X [79] and the range-separated double hybrid functional ω B2PLYP [80]. Although these functionals systematically overestimate excitation energies, the relative values among different states and different molecules are generally reliable [75]. Thus, we compare TDDFT excitation energies of QAD derivatives with QAD and rely on qualitative trends to gain valuable insight. We note that with such functionals, CT states may be over-corrected to become erroneously higher in energy than valence states for some molecules [75]. Therefore, validation against high-level quantum chemistry methods is still recommended for QAD.

For validation purposes, TDDFT results for QAD, QAD-3Ph, and QAD-7Ph were benchmarked with respect to experimental values and high-level quantum chemistry calculations using the domain-based local pair natural orbital (DLPNO) implementation [63, 64] of the similarity transformed equation of motion coupled cluster theory with single and double excitations (DLPNO-STEOM-CCSD) [65]. The equation of motion (EOM) approach is an extension of the ground state coupled cluster (CC) theory to compute excitation energies by a linear operator on the similarity transformed Within STEOM-CCSD, a second similarity transformation is Hamiltonian [81]. performed, which reduces the computational cost and yields more accurate excitation energies than EOM-CCSD. The DLPNO technique [63, 64] enables computing the ground state CC energies for large molecules. It has been demonstrated that the DLPNO-STEOM-CCSD approach does not lose any significant accuracy relative to its canonical counterpart [82, 67, 83, 84, 81, 85]. In particular, the mean absolute error (MAE) of DLPNO-STEOM-CCSD compared to experiments for CT excitations of various TADF molecules has been found to be only 0.09 eV [75].

As shown in Figure 2(a), the MAE of DLPNO-STEOM-CCSD compared to experiments for QAD, QAD-3Ph, and QAD-7Ph is about 0.11 eV, consistent with previous results for a benchmark set of other TADF molecules [75]. TDDFT is benchmarked here using the global hybrid functional B3LYP [86], the long-range corrected (LC) hybrid functionals LC-BLYP [78] and ω B97X [79], and the range-separated double hybrid functional ω B2PLYP [80]. The latter three functionals have 100% Fock exchange in the long range and range separation parameters of about 0.30 $bohr^{-1}$. Tabulated energies are provided in the Supplementary Material. Due to the large fraction of Fock exchange included in the range-separated hybrid and double-hybrid functionals, their MAEs are over 0.80 eV, considerably larger than that of TDDFT@B3LYP. Despite producing absolute S_1 energies in closer agreement with experiments and DLPNO-STEOM-CCSD, the performance of TDDFT@B3LYP strongly depends on the character of specific excited states (CT vs. valence) and is not systematic [75]. In addition, TDDFT@B3LYP yields incorrect S_1 energy ordering

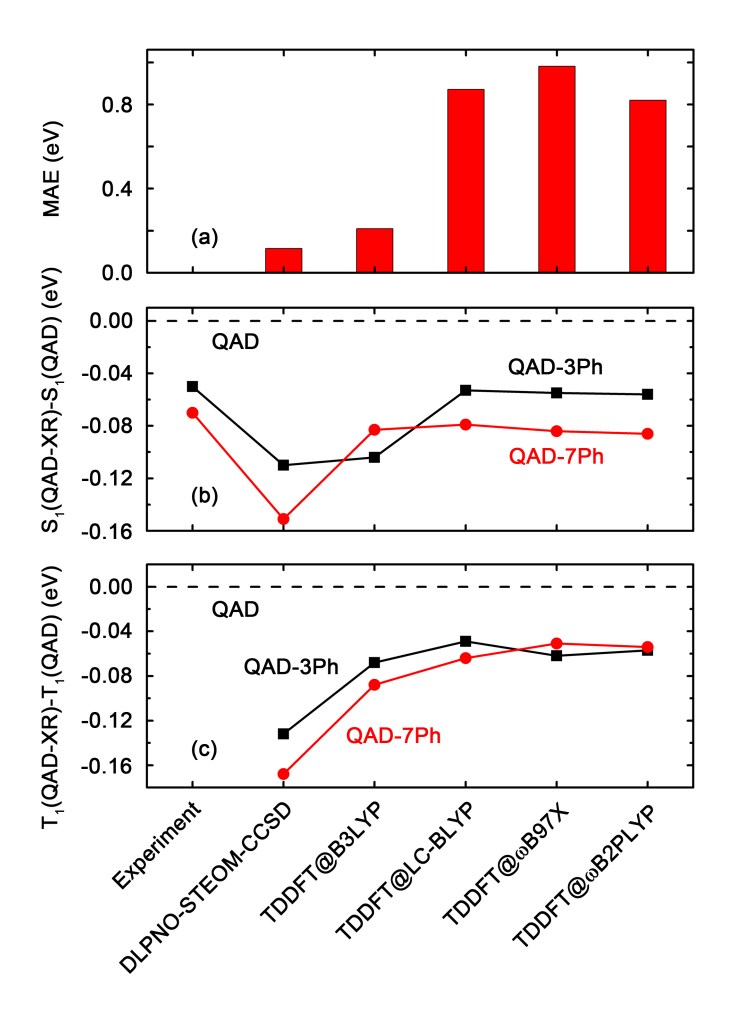


Figure 2. (a) MAEs of DLPNO-STEOM-CCSD and TDDFT referenced to experiments [44, 45] for the S_1 energies of QAD, QAD-3Ph, and QAD-7Ph. (b) S_1 and (c) T_1 energies of QAD-3Ph (black) and QAD-7Ph (red) compared to QAD. Tabulated excitation energies are provided in the Supplementary Material.

between QAD-3Ph and QAD-7Ph, as shown in Figure 2(b). This erroneous S_1 energy ordering of QAD-3Ph vs. QAD-7Ph has also been reported by others [45]. In contrast, the experimentally observed trends in the relative S_1 energies of QAD, QAD-3Ph, and QAD-7Ph [44, 45] are accurately reproduced with the LC-BLYP, ω B97X, and ω B2PLYP functionals. We further compare the T_1 energies obtained with these three functionals to DLPNO-STEOM-CCSD in Figure 2(c). Erroneous ordering of T_1 energies of QAD-3Ph and QAD-7Ph is found with the ω B97X and ω B2PLYP functionals. Moreover, with the ω B2PLYP functional, the triplet state dominated by the transition from HOMO to LUMO is energetically over-corrected to be the third lowest excited state, T_3 , instead of T_1 , for QAD, QAD-3Ph, and QAD-7Ph. Only the LC-BLYP functional provides a qualitatively correct description of the spectral composition of excited states and correct relative energy ordering of excited states between QAD and its derivatives. Therefore, we proceed to use TDDFT@LC-BLYP for the study of chemical modification of QAD and our discussion is restricted to qualitative trends between different molecules.

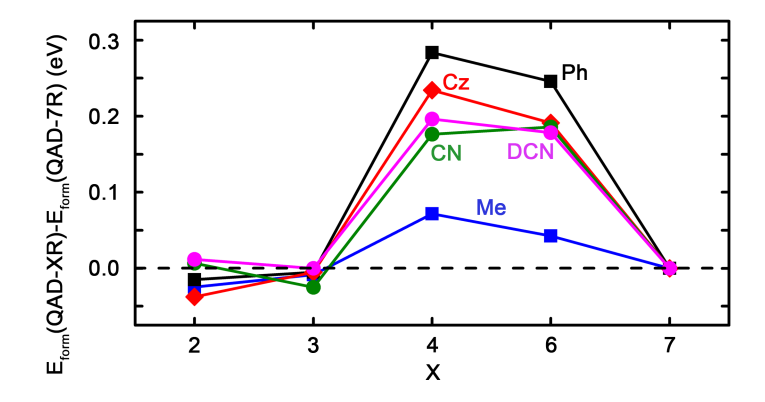


Figure 3. Formation energies of QAD-XR referenced to QAD-7R.

3.2. Substituent groups

We consider five chemical groups, methyl (Me), phenyl (Ph), carbazole (Cz), cyano (CN), and 1.3-dicynobenzene (DCN), and five substitution sites, denoted as 2, 3, 4, 6, and 7 in Figure 1(f). The Me group is electron donating because electrons withdrawn from the H atoms create excess negative charge over the C atom. The Ph group is electron withdrawing by induction, but anyl groups can be either electron donating or withdrawing by resonance, depending on where they are attached. The Cz, CN, and DCN groups are commonly used in donor-acceptor TADF molecules [9, 17, 87, 88]. Cz is a widely used strong donor moiety thanks to its advantages, including inexpensive starting materials, ease of functionalization at the N atom, several linkage positions, and the conformational stability of aromatics [17]. The CN group is widely employed as a strong acceptor moiety, often in the form of CN substituted aromatics, such as DCN [9, 89, 90, 91]. Both CN and DCN are considered here because their conjugation may be different. The linear CN group adopts a coplanar conformation with the QAD framework. In contast, the DCN group is twisted, possibly breaking its conjugation with the QAD skeleton. The substitution of CN group on MR-TADF molecules has been used in developing full-color TADF chromophores [92]. For example, an MR-TADF molecule has been red-shifted from emitting yellow light to emitting orange-red light by attaching a CN group on a C atom contributing to the LUMO [92]. Here, substitution positions contributing to both HOMO, such as 3 and 7, and LUMO, such as 2, 4, and 6, are investigated. The theoretical case study of QAD substituted with different groups and on different positions may be informative for chemical modification of other MR-TADF chromophores.

To assess the relative stability and the prospects of synthesizing the proposed compounds, we begin by analyzing the formation energies of QAD derivatives, shown in Figure 3. Relative formation energies may affect the yields of different products in experimental synthesis. For each substituent, R, the formation energy of the derivative QAD-7R is referenced to zero because substituents are usually experimentally attached to positions 3 and 7, the para-position to the central N, which contribute to the HOMO.

For example, [1,1'-biphenyl]-4-amine, where a Ph and an amine are para-substituted on a benzene ring, was used as a reactant in the synthesis of Ph-substituted QAD, yielding 53% QAD-3Ph and 27% QAD-7Ph [45]. In comparison, p-toluidine, where a Me and an amine are para-substituted on a benzene ring, was also used in the synthesis of Me-substituted QAD, yielding a 1:1 mixture of QAD-3Me and QAD-7Me [93]. This implies that, although a considerable amount of QAD-3R and QAD-7R may be obtained simultaneously owing to their similar formation energies, the substituent group may also affect the yields. In contrast, if the substituent is attached on a meta-position to the N, such as 2, 4, and 6, the formation energy varies significantly. The formation energies of QAD-4R and QAD-6R are larger than the other three, especially QAD-2R, owing to the repulsion of the O atom. If a substituent is expected to be attached on an atom contributing to the LUMO, position 2 may be superior to 4 and 6 in terms of relative stability and product yield. The steric hindrance of the O atom is also reflected in the dependence of the formation energy on the size of the substituent. The small Me results in lower formation energies at positions 4 and 6 relative to 7, compared to bulkier groups. Therefore, if a large chemical group is employed to functionalize QAD, positions 2, 3, and 7 may be energetically favored. It is noted that many donor-acceptor TADF molecules comprise ortho-substituted phenyl rings [94]. Therefore positions 4 and 6 are also investigated despite their proximity to the O atom. All five substituents and five substitution positions are calculated to provide a theoretical insight into designing MR-TADF chromophores, although some of these compounds may be difficult to synthesize experimentally.

3.3. Frontier orbitals

As a first stage of assessing the proposed compounds as TADF chromophores, we visually inspect the DFT orbitals to investigate the effect of side group substitutions on the spatial distribution of the frontier orbitals. Ideally, the substituents should enable tuning the chromophore's color without changing the nature of the TADF from MR to donor-acceptor. Figure 4 shows the frontier orbitals of QAD derivatives. The spatial distribution of the frontier orbitals depends on the character of the substituent. Of all substituents, only the strong donor, Cz, turns QAD into a donor-acceptor molecule, regardless of the substitution position. The HOMO and LUMO are spatially separated and localized on the Cz moiety and QAD skeleton respectively. Due to the rotatable single bond between Cz and QAD, the optimal molecular geometries of the ground state and excited states may differ more than in the rigid unsubstituted QAD, which may lead to a broadened emission peak and poor color purity. [95, 96, 97, 98] This agrees with the experimental observation of a very large FWHM in QAD-DAd, whose HOMO is located on the two DMAC strong donor moieties [44]. Thus, functionalization with strong electron donating groups may be detrimental to the performance of MR-TADF molecules. The other groups studied here, including the weak electron donating group Me and the strong electron withdrawing groups CN and DCN, do not alter the

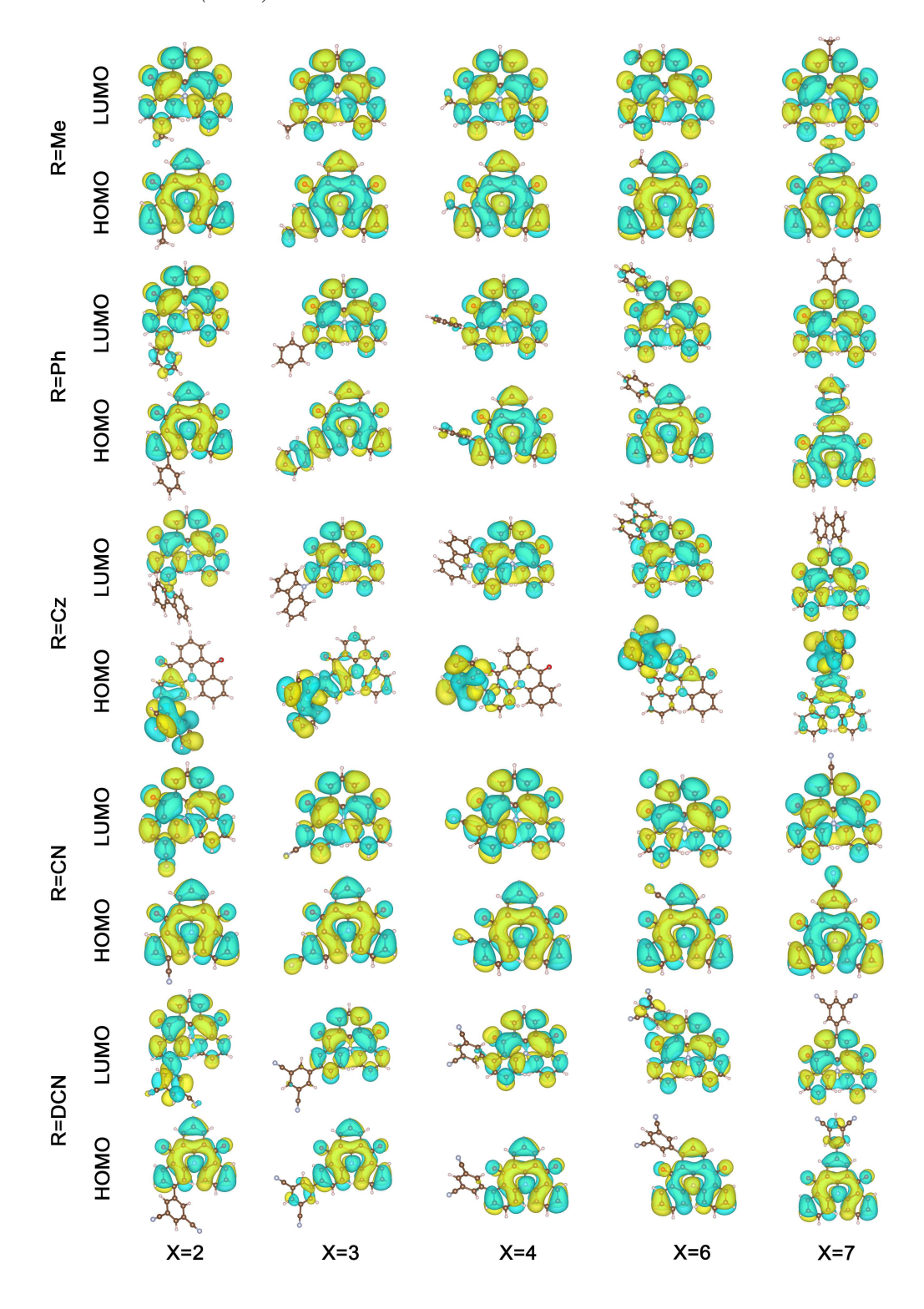


Figure 4. Frontier orbitals of QAD-XR obtained with DFT@LC-BLYP. The molecular orbitals are visualized with an isosurface value of 0.014 au.

distribution of the frontier orbitals on the QAD skeleton. Hence, these QAD derivatives are still considered as candidate MR-TADF chromophores.

For Me, Ph, CN, and DCN, whether the frontier orbitals are extended to the substituents depends on the electron donating/withdrawing character of the atom, to which the substituents are attached. For example, the C atoms in positions 3 and 7 of QAD act as electron donors and contribute to the HOMO. Thus, the HOMOs are extended from these atoms to the Me, Ph, CN, and DCN substituent groups, whereas the LUMOs are still localized on the QAD skeleton [55]. This is observed even for the strong withdrawing groups, CN and DCN. These acceptors typically contribute to the LUMOs. However, when attached to the 3 and 7 positions, they contribute to the HOMOs of QAD-3R and QAD-7R. It is noted that CN is coplanar with the QAD skeleton and DCN is twisted. The torsion angle between DCN and QAD somewhat breaks π conjugation between them and slightly limits the HOMO distribution on DCN in QAD-3DCN and QAD-7DCN. In contrast to QAD-3R and QAD-7R, the LUMOs of QAD-2R are extended to the substituent groups, whereas the HOMOs are not, due to the electron withdrawing character of the C atom in position 2. The C atoms in positions 4 and 6 have a similar electron withdrawing character to the C atom in position 2. However, they are close to the O atom of QAD, which creates steric hindrance. This results in larger torsion angles between QAD and the Ph and DCN substituents attached to positions 4 or 6, compared to other substitution positions, breaking the π conjugation. Thus, the spatial extension of the frontier orbitals to Ph and DCN attached to positions 4 and 6 is relatively small. Torsion angles between the QAD skeleton and substituents are provided in the Supplementary Material.

We now turn to investigate the effect of chemical substitutions on the frontier orbital energies of the QAD derivatives. Figure 5 shows the frontier orbital energies of QAD-XR, referenced to unsubstituted QAD. Tabulated orbital energies are provided in the Supplementary Material. Generally, the HOMO and LUMO energies of Me and Ph substituted QAD derivatives are within 0.15 eV of QAD, due to the relatively weak electron donating/withdrawing character of Me and Ph. The HOMOs of QAD-XCz are 0.19 to 0.52 eV higher than QAD because they are contributed by the Cz strong donor instead of the donating atoms on the QAD skeleton. The HOMO and LUMO energies of CN and DCN substituted QAD derivatives are both significantly decreased. Although they originate from the same atoms as in the parent QAD, they are energetically lowered by attached acceptors. It is noted that despite the similar behavior of the CN and DCN substituted derivatives, the difference between the LUMO energies of QAD-6CN and QAD-6DCN is 0.14 eV. This demonstrates that DFT and TDDFT calculations can aid the molecular design of MR-TADF chromophores by capturing the qualitative differences in the frontier orbital spatial distributions and the quantitative trends in their energies, induced by chemical modifications.

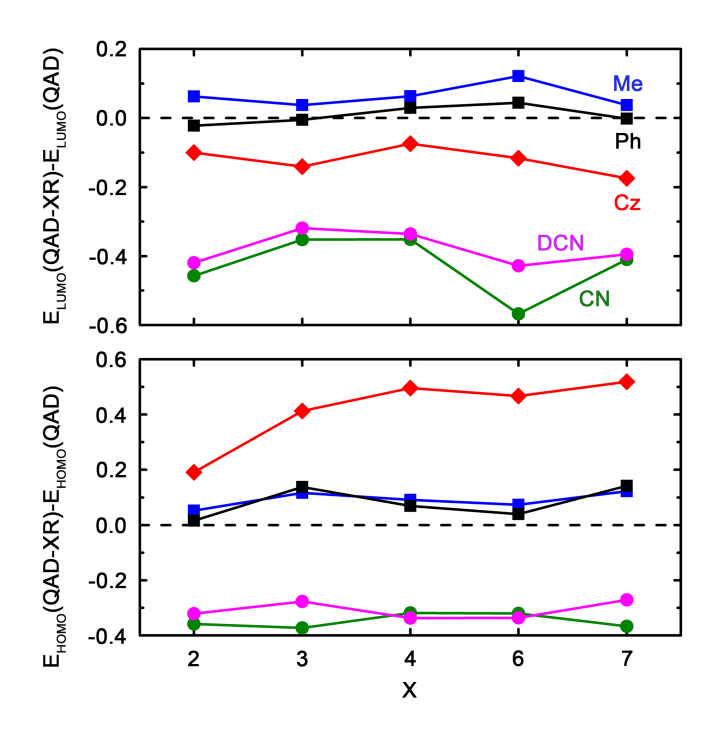


Figure 5. The change in the DFT@LC-BLYP HOMO (lower panel) and LUMO (upper panel) energies of QAD-XR, referenced to QAD, in units of eV. Tabulated orbital energies are provided in the Supplementary Material.

3.4. Excited states

If proposed derivatives are deemed likely to be synthesizable, and their ground state orbital energies are modified while retaining their MR-TADF nature, a detailed investigation of their excited states should be performed. Figure 6(a) shows the HOMO-LUMO energy gaps of Me, Ph, CN, and DCN substituted QAD derivatives referenced to QAD. For the most part, the trends in the S_1 energies in panel (b) track the changes in HOMO-LUMO gaps for all substituents, implying that side groups modify the excitation energies of QAD mainly through the molecular orbital energies. The S_1 energies of QAD-4Ph and QAD-6Ph are outliers, as they are lower than expected based on the HOMO-LUMO gaps. This is because upon Ph substitution in positions 4 and 6, the second lowest singlet excited state, S_2 , of QAD-(4/6)Ph, localized on the carbonyl groups, becomes lower in energy than the S_1 of QAD, which is dominated by the transition from HOMO to LUMO, as illustrated in Figure 7. A change of the energy ordering of the two lowest singlet excited states is also found in QAD-4CN. In addition to the change of the energy ordering, the spatial distribution of the three lowest singlet excited states also changes. The excited states distributed symmetrically on both carbonyl groups of QAD become localized exclusively on only one carbonyl group of QAD-4Ph. The excited state dominated by the $HOMO \rightarrow LUMO$ transition is mostly unchanged, except for an increased spatial distribution on the carbonyl group near the Ph.

The T_1 states of Me, Ph, CN, and DCN substituted QAD derivatives are still

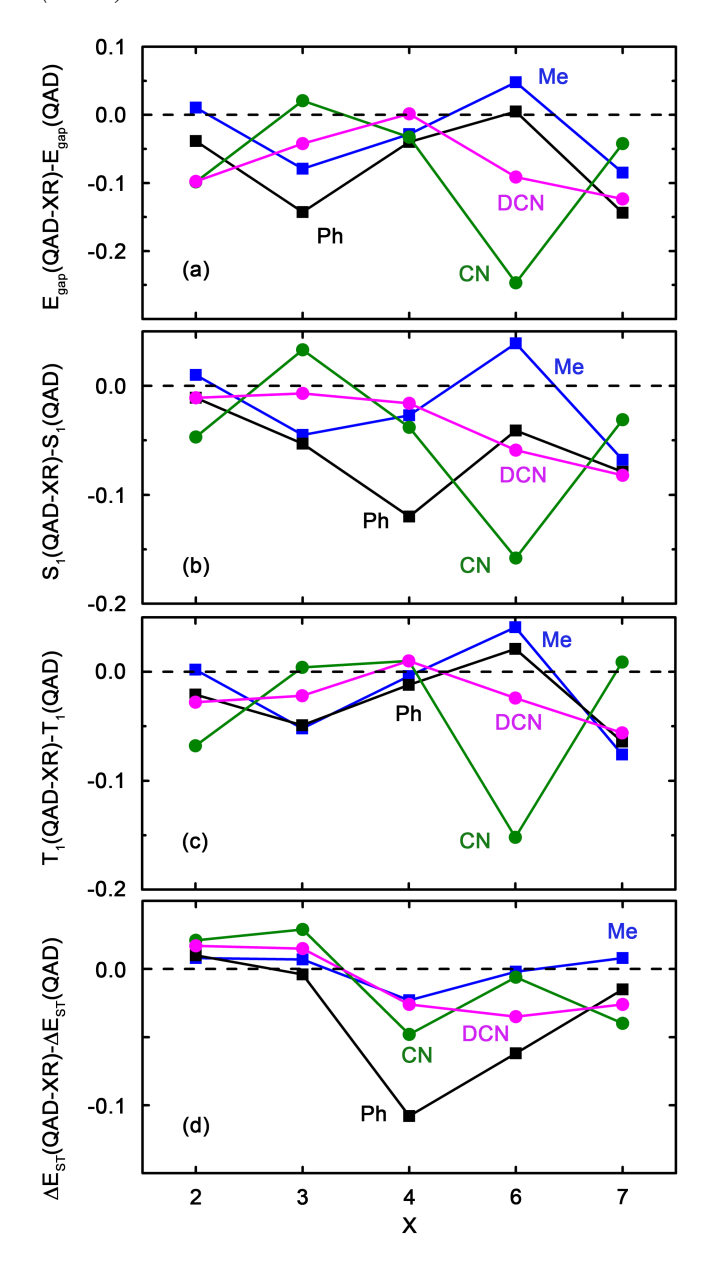


Figure 6. (a) The DFT@LC-BLYP HOMO-LUMO gap, (b) TDDFT@LC-BLYP S_1 , (c) TDDFT@LC-BLYP T_1 , and (d) TDDFT@LC-BLYP ΔE_{ST} of QAD derivatives referenced to QAD. The energy unit is eV. Tabulated excitation energies are provided in the Supplementary Material.

dominated by the $HOMO \rightarrow LUMO$ transition. This is reflected in the contribution of the $HOMO \rightarrow LUMO$ transition to T_1 , provided in the Supplementary Material, as well as in the T_1 energies, shown in Figure 6(c). The trends in the T_1 energies track the changes in the HOMO-LUMO gaps more closely than the S_1 energies. This analysis of the S_1 and T_1 excited states of QAD derivatives demonstrates the importance of TDDFT simulations in search of MR-TADF chromophores. Although Me, Ph, CN, and DCN substituted QAD derivatives are candidate MR-TADF chromophores based on the visual inspection of their ground-state frontier orbitals, their excited states may

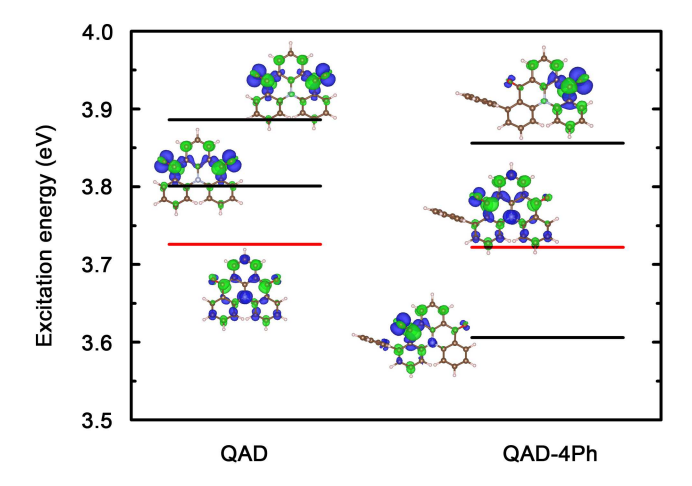


Figure 7. Energies of the three lowest singlet excited states for QAD (left) and QAD-4Ph (right). The excited states dominated by the transition from HOMO to LUMO are shown in red. The excited states localized on the carbonyl groups are shown in black. The electron density differences between the excited state and the ground state, obtained with TDDFT@LC-BLYP, are visualized for each state, with an isosurface value of 0.0018 au. The blue and green represent electron loss and gain.

not retain an MR-TADF nature, such as the S_1 of QAD-4Ph, QAD-6Ph, and QAD-4CN. Fortunately, TDDFT simulations reveal the relative decrease of their S_1 energies compared to the changes of the HOMO-LUMO gaps. In particular, although QAD-4Ph, QAD-6Ph, and QAD-4CN may no longer be considered as MR-TADF molecules, the relative decrease of their S_1 energies leads to the three smallest ΔE_{ST} in Figure 6(d), which may further facilitate TADF.

With the exception of QAD-4Ph and QAD-6CN, the S_1 energies of QAD derivatives are within 0.10 eV of QAD, as shown in Figure 6(b). Although this difference appears to be small, it is sufficient to noticeably change the color of a TADF chromophore. Of all the derivatives studied here, QAD-6CN exhibits the largest difference of S_1 from QAD, 0.16 eV. Applying this energy decrease to the experimental emission energy of QAD, 466 nm, yields 496 nm, corresponding to changing blue light to cyan light. This difference is consistent with experiments in which the attachment of a CN group has changed the emission of MR-TADF molecules from blue to green light and from yellow to orangered light, corresponding to decreasing S_1 by 0.08 and 0.12 eV, respectively [92]. The emission maximum of some MR-TADF molecules may be too high in energy for OLEDs, such as the 398 nm of DABOA, shown in Figure 1(a). Chemical modification may redshift their emission peaks to visible light for applications in OLEDs. It is noted that, a small energy decrease, such as a 0.10 eV through side group substitution, is enough to shift the emission peak of DABOA to blue light. However, chemical modification may not be sufficient, if the emission peak of an MR-TADF molecule is much higher in energy than the visible region, or a very large shift of the S_1 energy within the visible region is required to change the light color. Therefore, based on our analysis, chemical modification may be useful for fine tuning the emitted light around the color of the

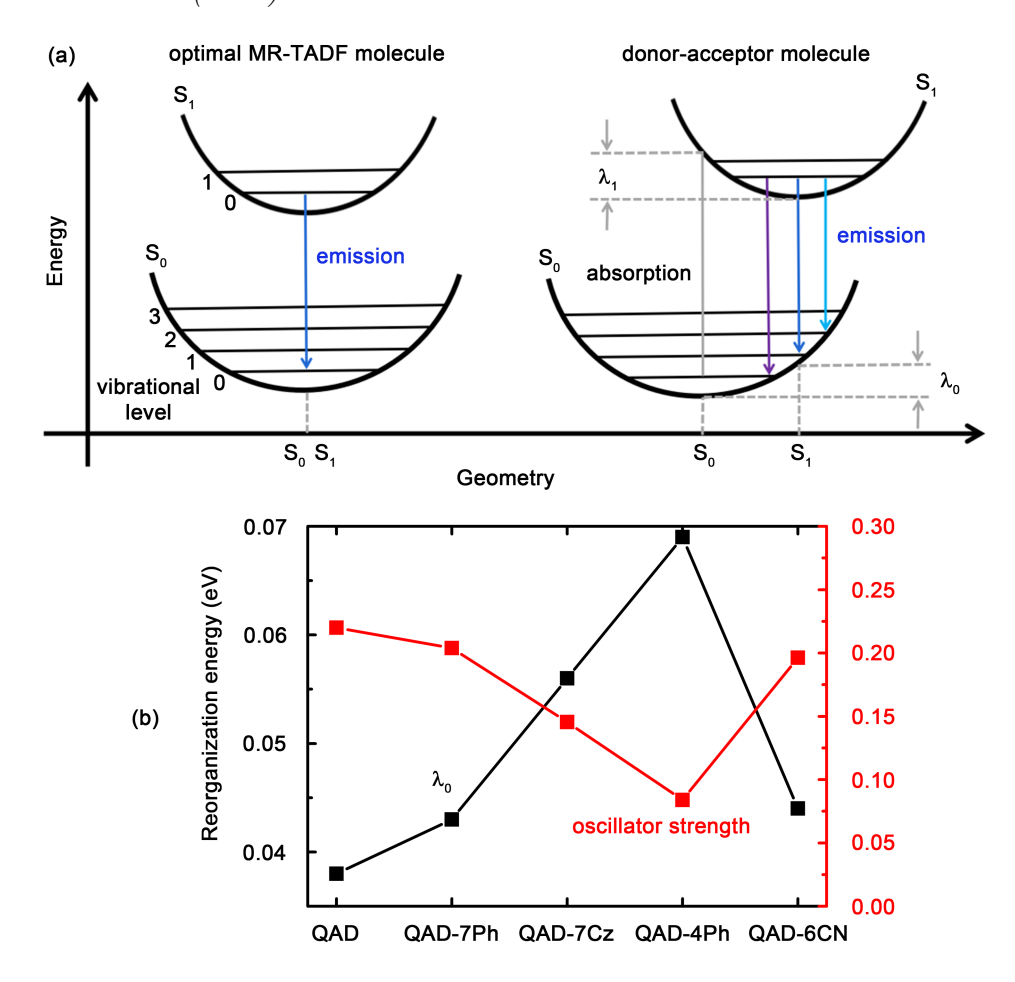


Figure 8. (a) Profiles of an optimal MR-TADF chromophore (left) and a donor-acceptor chromophore (right). Vibrational energy levels are indicated by numbers. λ_0 and λ_1 are the ground-state and excited state reorganization energies. (b) Reorganization energies (black) of QAD, QAD-7Ph, QAD-7Cz, QAD-4Ph, and QAD-6CN, obtained with the ω B97X-D functional and oscillator strength of the S_1 states (red), obtained with the LC-BLYP functional. Tabulated values of λ_0 , λ_1 , and oscillator strength are provided in the Supplementary Material.

parent MR-TADF compound, consistent with experimental observations [92].

Next, we assess emission color purity of QAD derivatives. The FWHM generally stems from geometry relaxation and vibrational broadening, as illustrated in Figure 8(a). The FWHMs of the emission and absorption peaks are determined by the ground-state reorganization energy, λ_0 , and the excited state reorganization energy, λ_1 . [96, 97, 98, 99, 100, 101]. Owing to the conformational rigidity of an optimal MR-TADF molecule, the difference between the relaxed S_0 and S_1 geometries is negligible. As a result, the emission occurs between the $\mathbf{0}$ vibrational energy levels of the ground state and the excited state. In contrast, the spatial distribution of the electron density in the ground state and in the excited state of donor-acceptor chromophores is significantly different due to the charge-transfer excitation character [102]. This, together with the rotatable bond between donor and acceptor moieties, leads to significantly different

relaxed S_0 and S_1 geometries. Owing to the large geometry difference, more vibrational energy levels are involved in emission, broadening the emission peak. Therefore, the emission FWHM may be related to the ground-state reorganization energy, λ_0 . It is noted that the contributions of normal vibration modes to reorganization energies may be analyzed to further demonstrate the source of FWHM. Peng et al. developed the thermal vibration correlation function (TVCF) formalism[103], which is taken into account in the activation energy of TADF, $\Delta G[101]$. ΔG is predicted to be a more appropriate descriptor of donor-acceptor TADF chromophores instead of ΔE_{ST} because of the vibration relaxation. Despite the in-depth understanding of the normal vibration modes, the reorganization energies are enough for the evaluation of the FWHM. Figure 8(b) shows the reorganization energies of representative molecules. The parent compound, QAD, is a typical MR-TADF molecule with a very low reorganization energy. QAD-7Ph is also an MR-TADF molecule, but its HOMO is extended to the Ph substituent (see Figure 4). QAD-7Cz is a donor-acceptor chromophore with a rotatable bond between the donor and acceptor moieties. Substitutions on position 7 are relatively easy to perform experimentally because the steric hindrance of the O atom is avoided. Upon Phenyl substitution on position 7 of QAD, λ_0 slightly increases. In comparison, λ_0 of QAD-7Cz is increased by as much as 50% with respect to QAD, considerably broadening the emission peak. This analysis agrees with the experimentally observed high color purity of the MR-TADF chromophores QAD-3Ph and QAD-7Ph, and the poor color purity of the donor-acceptor chromophore QAD-DAd [44, 45].

Using QAD, QAD-7Ph, and QAD-7Cz as references, we evaluate the color purity of the two best candidates, QAD-4Ph and QAD-6CN in Figure 8(b). QAD-4Ph stands out as having the lowest energy barrier to overcome in RISC, ΔE_{ST} . QAD-6CN has the largest S_1 energy change compared to QAD. QAD-4Ph exhibits a λ_0 higher than its isomer QAD-7Ph, and even higher than the donor-acceptor molecule QAD-7Cz. Although QAD-4Ph has the smallest ΔE_{ST} , its emission peak may be considerably broadened. Even worse, its oscillator strength of the S_1 state in Figure 8(b) is smaller than half of the QAD, reducing the quantum efficiency of radiation. The difference in oscillator strength for QAD-4Ph possibly results from the energy ordering change of the two lowest singlet states in Figure 7. The oscillator strength of the S_2 state of QAD-4Ph, dominated by the $HOMO \rightarrow LUMO$ transition, is 0.22, similarly to the S_1 state of QAD. In terms of the light color and the color purity, QAD-6CN is a promising new MR-TADF candidate. The chemical substitution changes the emission color of QAD from blue to cyan, while retaining a similar reorganization energy to QAD-7Ph, whose color purity has been experimentally confirmed [45]. Furthermore, QAD-6CN has a similar ΔE_{ST} and a similar oscillator strength of the S_1 state to the parent MR-TADF chromophore, QAD.

4. Conclusion

In summary, we have used computer simulations to investigate the effect of chemical modification on the excited-state properties of an MR-TADF chromophore, as a strategy for expanding the available color range for applications in OLEDs. We considered the QAD parent compound functionalized with five substituents of different electron donating/withdrawing ability in different positions. First, we evaluated the DFT formation energies of all compounds as an indicator of the ease of synthesis. We find that substitutions on positions 4 and 6 are more difficult owing to the steric hinderance of the O atom, in particular for bulky side-groups.

Second, we examined the spatial distribution of the DFT frontier orbitals to assess whether the substituted compounds retain their MR-TADF functionality. We find that strong electron donating groups, such as Cz, shift the distribution of the HOMO, such that it is localized on the donor moiety rather than on the QAD skeleton. This turns QAD into a donor-acceptor chromophore and is thus detrimental to MR-TADF. Other substituents, including Me, Ph, CN, and DCN, may preserve the high color purity because the spatial distribution of the HOMO and LUMO over the QAD skeleton is retained.

Third, we used TDDFT based on the long-range corrected hybrid functional LC-BLYP to evaluate the excitation energies of the QAD derivatives. We examined the change in the S_1 excitation energy, which corresponds to the change in the emission color, and the difference between the S_1 and T_1 excitation energies, ΔE_{ST} , which corresponds to the energy barrier for TADF. We find that chemical modification changes the excitation energies of QAD derivatives mainly by changing the ground state frontier orbital energies. QAD-6CN exhibits the greatest change in color compared to the parent compound, followed by QAD-4Ph. QAD-4Ph is found to have the smallest ΔE_{ST} of the compounds studied here, which may further facilitate TADF, whereas QAD-6CN has a similar ΔE_{ST} to QAD. However, side-group substitution changes the energy ordering of the excited states of QAD-4Ph, such that the lowest singlet excited state is no longer dominated by a HOMO to LUMO transition, but by a transition localized on one carbonyl group. This effectively changes the MR-TADF functionality despite not appearing to be so based on the spatial distribution of the DFT HOMO and LUMO. This demonstrates the necessity of TDDFT analysis beyond the visual inspection of ground-state frontier orbitals.

Finally, we considered the reorganization energy, which corresponds to the color purity of TADF chromophores. The reorganization energy of QAD-4Ph is found to be significantly higher than that of QAD and of QAD-7Ph. Therefore, the increase in the reorganization energy may be attributed to the change in the nature of the S_1 excited state rather than the rotatable bond with the phenyl side group. Based on the reorganization energy, QAD-4Ph may exhibit a considerably broadened emission peak, prohibiting its application in high-resolution displays. The reorganization energy of QAD-6CN is similar to that of QAD-7Ph, which has been experimentally observed

to exhibit MR-TADF with high color purity.

We thus conclude that QAD-6CN stands out as a promising MR-TADF chromophore based on all the performance metrics considered here. It is predicted to exhibit efficient MR-TADF thanks to the low energy barrier to RISC, and high color purity, thanks to the low reorganization energy. It is expected to emit light with a lighter cyan hue compared to the blue color of QAD. The case study of QAD derivatives demonstrates that chemical modification of MR-TADF chromophores may change the color of their light emission and/or improve their TADF performance without decreasing their color purity. Similar computational studies may be helpful to the development of new MR-TADF chromophores for applications in full-color high-resolution OLED displays, as well as in solar-cells utilizing TTA upconversion.

Acknowledgments

The authors thank the Natural Science Foundation of Shandong Province, China (Grant No. ZR2020QB073). Work at CMU was supported by the National Science Foundation (NSF) Division of Materials Research through grant DMR-2021803. We thank Yang Guo from Shandong University for helpful discussions. This research used resources of the Argonne Leadership Computing Facility (ALCF), which is a DOE Office of Science User Facility supported under Contract DE-AC02-06CH11357 and of the National Energy Research Scientific Computing Center (NERSC), a DOE Office of Science User Facility supported by the Office of Science of the U.S. Department of Energy, under Contract DE-AC02-05CH11231.

Data availability statement

The data of this study are available in the article and in the Supplementary Material.

ORCID IDs

Xiaopeng Wang (0000-0001-6866-4864) and Noa Marom (0000-0002-1508-1312)

References

- [1] Hong G, Gan X, Leonhardt C, Zhang Z, Seibert J, Busch J M and Bräse S 2021 Adv. Mater. 33 2005630
- [2] Reineke S, Thomschke M, Lüssem B and Leo K 2013 Rev. Mod. Phys. 85 1245
- [3] Geffroy B, Le Roy P and Prat C 2006 Polym. Int. **55** 572–582
- [4] Tang C W and VanSlyke S A 1987 Appl. Phys. Lett. 51 913-915
- [5] Baldo M, Lamansky S, Burrows P, Thompson M and Forrest S 1999 Appl. Phys. Lett. 75 4-6
- [6] Baldo M, ThompSOn M E and Forrest S 2000 Nature 403 750–753
- [7] Xu H, Chen R, Sun Q, Lai W, Su Q, Huang W and Liu X 2014 Chem. Soc. Rev. 43 3259–3302
- [8] Parker C A and Hatchard C G 1961 Trans. Faraday Soc. 57(0) 1894–1904

- [9] Yang Z, Mao Z, Xie Z, Zhang Y, Liu S, Zhao J, Xu J, Chi Z and Aldred M P 2017 Chem. Soc. Rev. 46 915–1016
- [10] Tao Y, Yuan K, Chen T, Xu P, Li H, Chen R, Zheng C, Zhang L and Huang W 2014 Adv. Mater. 26 7931–7958
- [11] Wong M Y and Zysman-Colman E 2017 Adv. Mater. 29 1605444
- [12] Liu Y, Li C, Ren Z, Yan S and Bryce M R 2018 Nat. Rev. Mater. 3 1–20
- [13] Bryden M A and Zysman-Colman E 2021 Chem. Soc. Rev. **50** 7587–7680
- [14] Mahoro G U, Fernandez-Cestau J, Renaud J L, Coto P B, Costa R D and Gaillard S 2020 Adv. Opt. Mater. 8 2000260
- [15] To W P, Cheng G, Tong G S M, Zhou D and Che C M 2020 Front. Chem. 8 653
- [16] Han Z, Dong X Y and Zang S Q 2021 Adv. Opt. Mater. 9 2100081
- [17] Wex B and Kaafarani B R 2017 J. Mater. Chem. C $\mathbf{5}(34)$ 8622–8653
- [18] Fang F, Zhu L, Li M, Song Y, Sun M, Zhao D and Zhang J 2021 Adv. Sci. 8 2102970
- [19] Gómez-Bombarelli R, Aguilera-Iparraguirre J, Hirzel T D, Duvenaud D, Maclaurin D, Blood-Forsythe M A, Chae H S, Einzinger M, Ha D G, Wu T et al. 2016 Nat. Mater. 15 1120–1127
- [20] Zhu J, Liao Q, Huang H, Fu L, Liu M, Gu C and Fu H 2022 Cell Reports Physical Science 3 100686
- [21] Huang B, Chen W C, Li Z, Zhang J, Zhao W, Feng Y, Tang B Z and Lee C S 2018 Angew. Chem. Int. Ed. 130 12653–12657
- [22] Zhan L, Chen Z, Gong S, Xiang Y, Ni F, Zeng X, Xie G and Yang C 2019 Angew. Chem. Int. Ed. 131 17815–17819
- [23] Fang F, Yuan Y, Wan Y, Li J, Song Y, Chen W C, Zhao D, Chi Y, Li M, Lee C S et al. 2022 Small 18 2106215
- [24] Sun J W, Lee J H, Moon C K, Kim K H, Shin H and Kim J J 2014 Adv. Mater. 26 5684–5688
- [25] Kaji H, Suzuki H, Fukushima T, Shizu K, Suzuki K, Kubo S, Komino T, Oiwa H, Suzuki F, Wakamiya A et al. 2015 Nat. Commun. 6 8476
- [26] Singh-Rachford T N and Castellano F N 2010 Coord. Chem. Rev. 254 2560–2573
- [27] Goldschmidt J C and Fischer S 2015 Adv. Opt. Mater. 3 510–535
- [28] Gray V, Moth-Poulsen K, Albinsson B and Abrahamsson M 2018 Coord. Chem. Rev. 362 54–71
- [29] Ahmad W, Wang J, Li H, Ouyang Q, Wu W and Chen Q 2021 Coord. Chem. Rev. 439 213944
- [30] Xiao X, Tian W, Imran M, Cao H and Zhao J 2021 Chem. Soc. Rev. 50(17) 9686–9714
- [31] Wang X, Tom R, Liu X, Congreve D N and Marom N 2020 J. Mater. Chem. C 8(31) 10816–10824
- [32] Yanai N, Kozue M, Amemori S, Kabe R, Adachi C and Kimizuka N 2016 J. Mater. Chem. C 4(27) 6447–6451
- [33] Wang X and Marom N 2022 Mol. Syst. Des. Eng. 7(8) 889–898
- [34] Polgar A M and Hudson Z M 2021 Chem. Commun. 57 10675-10688
- [35] Chen W, Song F, Tang S, Hong G, Wu Y and Peng X 2019 Chem. Commun. 55 4375–4378
- [36] Endo A, Sato K, Yoshimura K, Kai T, Kawada A, Miyazaki H and Adachi C 2011 Appl. Phys. Lett. 98 083302
- [37] Shi Y, Ma H, Sun Z, Zhao W, Sun G and Peng Q 2022 Angew. Chem. Int. Ed.
- [38] Hirai H, Nakajima K, Nakatsuka S, Shiren K, Ni J, Nomura S, Ikuta T and Hatakeyama T 2015 Angew. Chem. Int. Ed. 54 13581–13585
- [39] Hatakeyama T, Shiren K, Nakajima K, Nomura S, Nakatsuka S, Kinoshita K, Ni J, Ono Y and Ikuta T 2016 Adv. Mater. 28 2777–2781
- [40] Matsui K, Oda S, Yoshiura K, Nakajima K, Yasuda N and Hatakeyama T 2018 J. Am. Chem. Soc. 140 1195–1198
- [41] Liang X, Yan Z P, Han H B, Wu Z G, Zheng Y X, Meng H, Zuo J L and Huang W 2018 Angew. Chem. Int. Ed. 130 11486–11490
- [42] Han S H, Jeong J H, Yoo J W and Lee J Y 2019 J. Mater. Chem. C 7 3082–3089
- [43] Kondo Y, Yoshiura K, Kitera S, Nishi H, Oda S, Gotoh H, Sasada Y, Yanai M and Hatakeyama T 2019 Nat. Photonics 13 678–682

- [44] Yuan Y, Tang X, Du X Y, Hu Y, Yu Y J, Jiang Z Q, Liao L S and Lee S T 2019 Adv. Opt. Mater. 7 1801536
- [45] Li X, Shi Y Z, Wang K, Zhang M, Zheng C J, Sun D M, Dai G L, Fan X C, Wang D Q, Liu W et al. 2019 ACS Appl. Mater. Interfaces 11 13472–13480
- [46] Hall D, Suresh S M, dos Santos P L, Duda E, Bagnich S, Pershin A, Rajamalli P, Cordes D B, Slawin A M, Beljonne D et al. 2020 Adv. Opt. Mater. 8 1901627
- [47] Wu X, Su B K, Chen D G, Liu D, Wu C C, Huang Z X, Lin T C, Wu C H, Zhu M, Li E Y et al. 2021 Nat. Photonics 15 780–786
- [48] Gao H, Shen S, Qin Y, Liu G, Gao T, Dong X, Pang Z, Xie X, Wang P and Wang Y 2022 J. Phys. Chem. Lett. 13 7561–7567
- [49] Madayanad Suresh S, Hall D, Beljonne D, Olivier Y and Zysman-Colman E 2020 Adv. Funct. Mater. 30 1908677
- [50] Jiang P, Miao J, Cao X, Xia H, Pan K, Hua T, Lv X, Huang Z, Zou Y and Yang C 2022 Adv. Mater. 34 2106954
- [51] Lin S, Ou Q and Shuai Z 2022 ACS Mater. Lett. 4 487-496
- [52] Wang X, Liu X, Tom R, Cook C, Schatschneider B and Marom N 2019 J. Phys. Chem. C 123 5890–5899
- [53] Liu X, Tom R, Gao S and Marom N 2020 J. Phys. Chem. C 124 26134–26143
- [54] Liu X, Tom R, Wang X, Cook C, Schatschneider B and Marom N 2020 J. Phys. Condens. Matter. 32 184001
- [55] Lin S, Pei Z, Zhang B, Ma H and Liang W 2022 J. Phys. Chem. A 126 239–248
- [56] Jiang H and Zhang M Y 2020 SCIENTIA SINICA Chimica 50 1344–1362
- [57] Runge E and Gross E K U 1984 Phys. Rev. Lett. **52**(12) 997–1000
- [58] Liu W and Xiao Y 2018 Chem. Soc. Rev. 47(12) 4481–4509
- [59] Neese F 2012 WIREs Comput. Mol. Sci. 2 73–78
- [60] Chai J D and Head-Gordon M 2008 Phys. Chem. Chem. Phys. 10(44) 6615–6620
- [61] Arago J, Sancho-Garcia J C, Orti E and Beljonne D 2011 J. Chem. Theory Comput. 7 2068–2077
- [62] Weigend F and Ahlrichs R 2005 Phys. Chem. Chem. Phys. 7(18) 3297–3305
- [63] Riplinger C and Neese F 2013 J. Chem. Phys. 138 034106
- [64] Riplinger C, Sandhoefer B, Hansen A and Neese F 2013 J. Chem. Phys. 139 134101
- [65] Nooijen M and Bartlett R J 1997 J. Chem. Phys. 106 6441–6448
- [66] Hellweg A, Hättig C, Höfener S and Klopper W 2007 Theor. Chem. Acc. 117 587–597
- [67] Dutta A K, Saitow M, Demoulin B, Neese F and Izsák R 2019 J. Chem. Phys. 150 164123
- [68] Kümmel S 2017 Adv. Energy Mater. 7 1700440
- [69] Dreuw A and Head-Gordon M 2005 Chem. Rev. 105 4009-4037
- [70] Dreuw A and Head-Gordon M 2004 J. Am. Chem. Soc. 126 4007–4016
- [71] Vydrov O A and Scuseria G E 2006 J. Chem. Phys. 125 234109
- [72] Rohrdanz M A, Martins K M and Herbert J M 2009 J. Chem. Phys. 130 054112
- [73] Le Bahers T, Adamo C and Ciofini I 2011 J. Chem. Theory Comput. 7 2498–2506
- [74] Mester D and Kállay M 2022 J. Chem. Theory Comput. 18 1646–1662
- [75] Wang X, Gao S, Zhao M and Marom N 2022 Phys. Rev. Res. 4 033147
- [76] Casanova-Páez M and Goerigk L 2021 J. Chem. Theory Comput. 17 5165–5186
- [77] Loos P F, Comin M, Blase X and Jacquemin D 2021 J. Chem. Theory Comput. 17 3666–3686
- [78] Iikura H, Tsuneda T, Yanai T and Hirao K 2001 J. Chem. Phys. 115 3540-3544
- [79] Chai J D and Head-Gordon M 2008 J. Chem. Phys. 128 084106
- [80] Casanova-Páez M, Dardis M B and Goerigk L 2019 J. Chem. Theory Comput. 15 4735–4744
- [81] Berraud-Pache R, Neese F, Bistoni G and Izsák R 2020 J. Chem. Theory Comput. 16 564–575
- [82] Dutta A K, Saitow M, Riplinger C, Neese F and Izsak R 2018 J. Chem. Phys. 148 244101
- [83] Dutta A K, Neese F and Izsak R 2016 J. Chem. Phys. 145 034102
- [84] Dutta A K, Nooijen M, Neese F and Izsak R 2018 J. Chem. Theory Comput. 14 72–91
- [85] Schreiber M, Silva-Junior M R, Sauer S P A and Thiel W 2008 J. Chem. Phys. 128 134110

- [86] Stephens P J, Devlin F J, Chabalowski C F and Frisch M J 1994 J. Phys. Chem. 98 11623–11627
- [87] Zhang Q, Li B, Huang S, Nomura H, Tanaka H and Adachi C 2014 Nat. Photonics 8 326–332
- [88] Salah L, Etherington M K, Shuaib A, Danos A, Nazeer A A, Ghazal B, Prlj A, Turley A T, Mallick A, McGonigal P R et al. 2021 J. Mater. Chem. C 9 189–198
- [89] Park W J, Lee Y, Kim J Y, Yoon D W, Kim J, Chae S H, Kim H, Lee G, Shim S, Yang J H and Lee S J 2015 Synth. Met. 209 99–104 ISSN 0379-6779
- [90] Li B, Nomura H, Miyazaki H, Zhang Q, Yoshida K, Suzuma Y, Orita A, Otera J and Adachi C 2014 Chem. Lett. 43 319–321
- [91] Kretzschmar A, Patze C, Schwaebel S T and Bunz U H 2015 J. Org. Chem. 80 9126-9131
- [92] Liu Y, Xiao X, Ran Y, Bin Z and You J 2021 Chem. Sci. 12 9408-9412
- [93] Field JE, Hill TJ and Venkataraman D 2003 J. Org. Chem. 68 6071–6078
- [94] Chen X K, Bakr B W, Auffray M, Tsuchiya Y, Sherrill C D, Adachi C and Bredas J L 2019 J. Phys. Chem. Lett. 10 3260–3268
- [95] Santoro F, Lami A, Improta R, Bloino J and Barone V 2008 J. Chem. Phys. 128 224311
- [96] Qiu X, Tian G, Lin C, Pan Y, Ye X, Wang B, Ma D, Hu D, Luo Y and Ma Y 2021 Adv. Opt. Mater. 9 2001845
- [97] Liu F, Cheng Z, Wan L, Feng Z, Liu H, Jin H, Gao L, Lu P and Yang W 2022 Small 18 2106462
- [98] Kunnus K, Li L, Titus C J, Lee S J, Reinhard M E, Koroidov S, Kjær K S, Hong K, Ledbetter K, Doriese W B et al. 2020 Chem. Sci. 11 4360–4373
- [99] Park I S, Matsuo K, Aizawa N and Yasuda T 2018 Adv. Funct. Mater. 28 1802031
- [100] Peng Q and Shuai Z 2021 Aggregate 2 e91
- [101] Wang L, Ou Q, Peng Q and Shuai Z 2021 J. Phys. Chem. A 125 1468–1475
- [102] Tu Z, Han G, Hu T, Duan R and Yi Y 2019 Chem. Mater. 31 6665-6671
- [103] Peng Q, Niu Y, Shi Q, Gao X and Shuai Z 2013 J. Chem. Theory Comput. 9 1132–1143